# PROMPT NEUTRON DECAY MEASUREMENTS FOR AN ANNULAR HEU URANIUM METAL CASTING


John T. Mihalczo, Dan Archer, Michael Wright, and James A. Mullens

*Oak Ridge National Laboratory, P.O. Box 2008, Oak Ridge, Tennessee 37831-6010, mihalczojt@ornl.gov*



*Measurements were performed with a single annular, stainless-steel-canned casting of uranium (93.17 wt % $^{235}$U) metal (~18 kg) to provide data to verify calculational methods for criticality safety. The measurements used a small portable DT generator with an embedded alpha detector to time and directionally tag the neutrons from the generator. The center of the time and directional tagged neutron beam was perpendicular to the axis of the casting. The radiation detectors were 1 × 1 × 6-in.-long plastic scintillators encased in 0.25-in.-thick lead shields that were sensitive to neutrons above 1 MeV in energy. The detector lead shields were adjacent to the casting and the target spot of the generator was about 1.5 in. from the casting at the vertical center. The time distribution of the fission induced radiation was measured with respect to the source event by a fast (1GHz) time coincidence processor. The measurements described in this paper also include time correlation measurements with a time tagged spontaneously fissioning $^{252}$Cf neutron source, both on the axis and on the surface of the casting. Measurements with both types of sources are compared. Measurements with the DT generator closely coupled with the HEU provide no more additional information than those with the Cf source closely coupled with the HEU and are complicated by the time and directionally tagged neutrons from the generator scattering between the walls and floor of the measurements room and the casting while still above detection thresholds.*


## I. INTRODUCTION

A series of experiments with a single annular highly enriched uranium (HEU) metal casting was performed. The casting was a standard HEU storage casting located at the Y-12 National Security Complex and contained slightly less than 18 kg of uranium with 93.17 wt % $^{235}$U. The fission chain multiplication process was initiated by a small portable deuterium-tritium (DT) neutron generator or a $^{253}$Cf spontaneously fissioning neutron source, and the time behavior of prompt neutrons with respect to source emission and the time distribution of counts in one detector with respect to all other detectors were measured with plastic scintillation detectors. These detectors were sensitive to the fast neutrons above 1 MeV in energy and gamma rays without distinction. The neutron emission from the DT generator was time and directionally tagged by an alpha detector embedded in the generator. Thus, the alpha detector defined a beam of neutrons emitted by the DT generator in the direction of the casting. For the measurements with Cf, the neutron emission from the Cf source was time-tagged isotropic in all directions. These experiments were performed to provide data to benchmark methods to calculate prompt neutron time behavior. This paper describes the measurements and compares the results for both types of neutron sources. This work was supported by the Y-12 National Security Complex and the Department of Energy National Nuclear Security Administration.

## II. MATERIALS

The fissile material for these measurements was HEU metal with a $^{235}$U enrichment of 93.169 wt %. The $^{234}$U and $^{236}$U content was 0.997 and 0.457 wt %, respectively. The $^{238}$U content is the difference of these numbers from 100. The mass of the casting was 17,976 g, and the uranium metal contained 99.900 wt % uranium. The uranium metal was in the form of the standard HEU annular storage casting used at the Y-12 Complex. The outside diameter of the casting was 5.000 in.; the inside diameter was 3.500 in.[a] These dimensions, however, were not measured accurately and were assumed based on the dimensions of the graphite casting crucible and measurements of previous castings of this same type. The average impurity content was ~1000 ppm. The meniscus at the top of the casting caused by the solidifying of the melt was 1/16 in. deep. The density of the uranium metal was assumed to be 18.75 gm/cm$^3$.

The casting was contained in 0.025-in.-thick, 7.5-in.-high stainless steel (SS-304) cylindrical can for contamination control. The cylindrical can had an inside diameter of 3.0 in., large enough so that the Cf source

[a]Dimensions in this paper are given in units measured.

could be located on the axes of the casting and have stainless steel on the inside of the casting. The average outside diameter of the steel can with the casting inserted was 5.067 in., indicating a radial void of 0.009 in. The recessed lid welded on the bottom of the can resulted in the bottom of the uranium metal castings being 0.5 in. above the bottom of the outside of the can. To preclude water accumulation inside the annular can, the can rested on a 0.25-in.-thick A36 mild steel coaster that would allow water to drain out. So for the annular casting, the bottom of the HEU metal was ~0.5 in. above the 0.25-in. thick steel table.

## III. MEASUREMENT METHODS

Neutrons from the $^{252}$Cf spontaneously fissioning neutron source were time tagged by detecting the ionization from the fission products emitted from the Cf on one plate of a parallel-plate ionization chamber. Thus, time-tagged neutrons are emitted in all directions. A fraction of the neutron emission from the DT generator was detected by an embedded alpha detector, which measured the direction and time of emission of the alpha particle from the DT reaction. Since the neutron is emitted ~180º from the alpha particle in the DT reaction, the alpha particle detector can be use to time and directionally tag the neutron emission. Neutrons from the two types of source initiate fission in the HEU, and four small plastic scintillation detectors were used to measure the time behavior of the radiation emitted in the fission chain decay with respect to the source event. The fast (1 GHz) nuclear materials identification system (NMIS) processor record the time distribution of radiation emitted.[1] Several types of measurements were performed: (1) the time distribution of events in a detector with respect to a previous event in the same detector (autocorrelation function), which is the equivalent of the single detector Rossi-alpha measurement; (2) the time distribution of events in one detector with respect to a previous event in another detector (cross correlation function), which is equivalent to the two-detector Rossi-alpha measurements; (3) and the time distribution of events in a detector with respect to the source neutron emission, which is the equivalent of pulsed neutron measurements. All these provide the time decay of the fission chain population, which for low neutron multiplication can usually be represented by the sum of exponentials. Other quantities measured and not presented in this paper are the multiplets, which are the number of times n detections are recorded in each and the sum of all detectors in a time interval and higher-order correlations, which are the time distribution of events in any and all combinations of three detectors, including the Cf fission detector or the alpha detector for the DT generator. All these quantities are measured simultaneously by the NMIS processor for five input data channels.

## IV. MEASUREMENT HARDWARE

### IV.A. DT Generator

The small portable DT generator, provided by Oak Ridge National Laboratory (ORNL) for the measurements was a Thermo Fischer Scientific Corp. API120 with an embedded YAP scintillation detector for alpha detection.[2] The light from scintillation in the YAP was transmitted through a fiber-optic face plate to a photomultiplier tube (PMT) for detection of the light from the alpha particle's interaction in the YAP scintillator. The generator, including power supplies, weights 30 lb and uses ~50 watts of electrical power—it is basically a 3-in.-outside diameter (OD), 35-in.-long grounded pipe, as shown in Fig. 1. The generator has an ORTEC photomultiplier tube mounted adjacent to the outside of the fiber-optic face plate on which the YAP scintillator was mounted.

The time-tagged neutron beam from the generator was a fan-shaped beam produced by inserting an aperture between the photomultiplier tube and the outside of the fiber optic face plate. The aperture was a 52-mm-wide slit in the horizontal direction and was 11 mm high. The electronics for alpha detection was such that ~3% of the alpha triggers were false for the slit aperture. The percentage of the alphas impinging on the YAP scintillators that were counted was ~85%. The shape of the time-tagged neutron beam from this aperture was measured 85 cm from the target production in the generator, (see Figs. 2 and 3). The time-tagged neutron beam has a full width at half maximum of 11º in the 11-mm direction. For this measurement, the slit was rotated 90º so the measurement could be easily performed with a horizontally scanning apparatus. For the measurement of the beam profile in the long dimension, the slit was horizontally located. The time-tagged neutron beam is full width at half maximum of ~40º in the horizontal direction. The neutron beam is shifted because of the momentum of the accelerated ions in the accelerator (minus angle in direction of acceleration of the beam). For the measurements with the casting, the casting was centered in the time and directionally tagged neutron beam, both horizontally and vertically. The measurement of the shape of the time-tagged neutron beam is necessary for proper calculations of the measured results.

### IV.B. Cf Source

The Cf source was approximately 0.55 µg of $^{252}$Cf and had a spontaneous fission rate of ~330,000 fissions per second. The design of the Cf ionization chamber for the detection of Cf fission has been described.[3] The time-tagged neutrons from this source are emitted in all directions. When the source was on axis of the casting, it

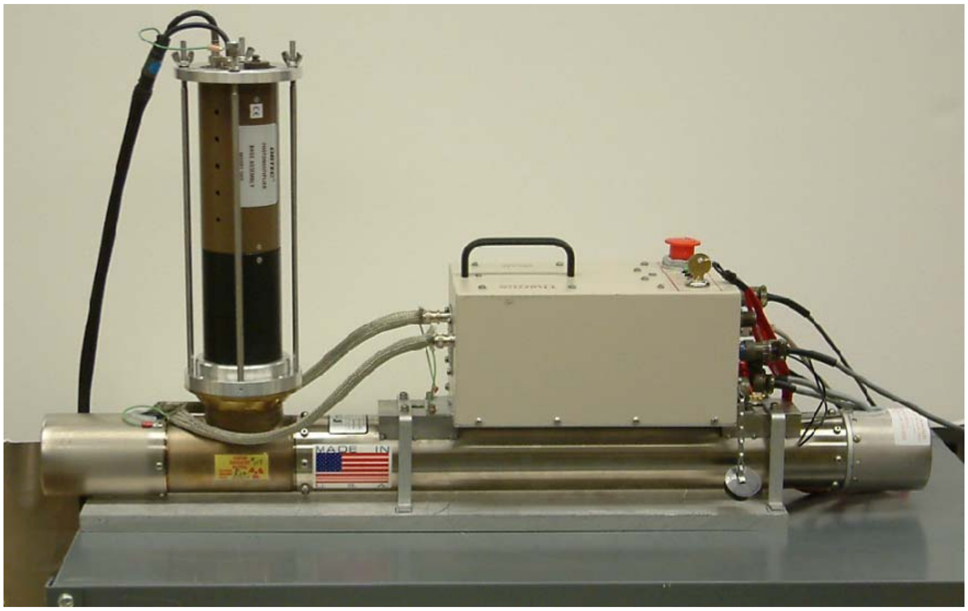


Fig. 1. The DT generator with an ORTEC base and PMT for alpha detection attached.

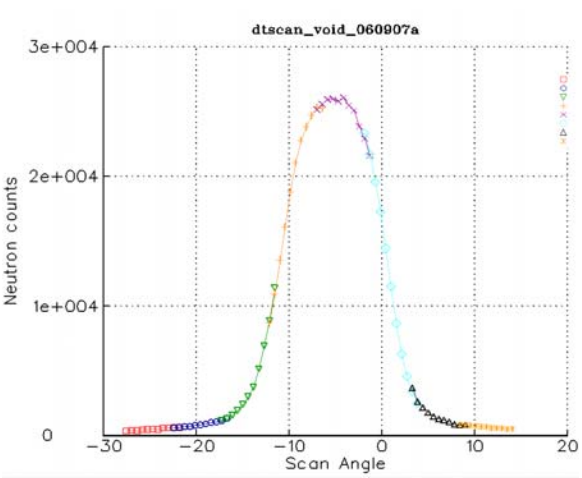


Fig. 2. Neutron counts as a function of angle across the slit aperture in the 11-mm vertical direction.

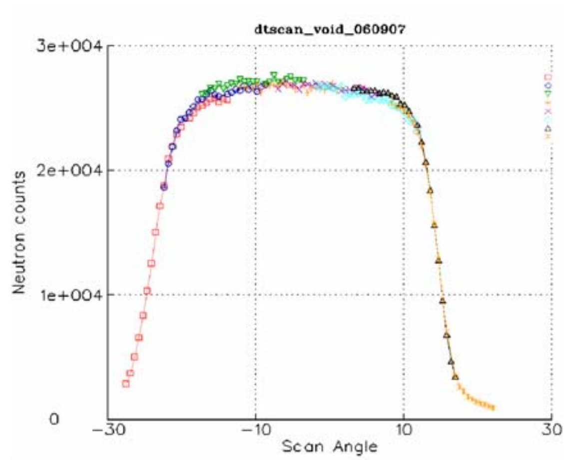


Fig. 3. Neutron counts as a function of angle across the slit aperture in the 52-mm horizontal direction.

was 3.00 in. up from the bottom of the casting. This source was also located in some measurements adjacent to the outer surface of the casting can. The spontaneous fission detection system for the Cf source was such that it detected a small number of false triggers from alpha particle detection in the radioactive decay of $^{252}$Cf. This spontaneous alpha decay for Cf is a factor of ~30 more numerous than for spontaneous fission, thus some of the Cf triggers were false and not related to the emission of neutrons. Second- and third-order correlation measurements determined that ~1% of the Cf triggers were false.

In all measurements, the Cf source was located 3.25 in. above the steel table. For internal locations, the 1-cm-diam. Cf deposit was horizontal. For external locations, most of the time the Cf deposit was vertical and adjacent to the surface of a can.

### IV.C. Radiation Detectors

A wide variety of radiation detectors were considered for these measurements. It was decided that the smaller the detector and the closer it was to the castings, the less the measured prompt decay would be affected by detector effects and neutron time of flight effects to the detectors. These plastic scintillation neutron detectors reflect neutrons and could change the prompt decay of the fission chains if the detectors were large. The smaller the detector, the less the light propagation effects occur in the detector. Four 1 × 1 × 6-in.-long plastic scintillators with the long dimension parallel to axes of the castings and adjacent to the outer surface of the casting cans were used in the measurements. The detectors were enclosed in 0.25-in.-thick lead shields on four 1 × 6 in. surfaces and on the 1 × 1 in. bottom surface. The bottom surface of the lead shield was adjacent to the steel table.

The neutron detection efficiency as a function of energy was obtained as a function from a time-of-flight measurement in air where the Cf source was separated 110 cm from the detectors, and the centers of both the source and the detectors were 120 cm above the floor. These measurements were performed with the lead shields around the detectors. This information is also necessary for comparison of measurement with calculations. These measurements also obtained the energy threshold for neutron detection. These measurements were performed daily before measurements with HEU and appropriate adjustments were made to ensure reproducibility of the measurements. The efficiency per incident neutron can be determined from (1) the time distribution of neutrons after Cf fission, which gives the neutron energy and the number of detections at a given energy, (2) the known number of neutrons per Cf fission, (3) the known neutron energy distribution of neutrons from Cf, (4) the solid angle subtended by the detector, and (5) the total measured number of Cf fissions in the detection efficiency measurement. A typical time distribution of counts as a function of time after Cf fission is given in Fig. 4. In all time distributions given in this paper, the accidental coincidences have been subtracted. In these measurements, the long dimension of the detector was perpendicular to a line between the source and the center of the detector.

The initial peak is from gamma rays that arrive at the detectors at ~3.6 ns. This peak is followed by the neutron peak at 50 ns whose shape is determined by the spectrum of neutron from Cf fission. After 100 n, neutrons reflected from the floor are detected. The data of Fig. 4 are used to obtain the detection efficiency as a function of energy and the energy threshold for detection of neutrons. Typical plots of neutron efficiency per incident neutron impinging on the detector are given in Fig. 5. The efficiency increase between 1 and 2 MeV stays constant for a small range of energies and then decreases after 3 MeV because of the reduction of the hydrogen cross section with energy because many of the events in the detector are neutron scattering by hydrogen. The neutron thresholds and the maximum detection efficiencies were 1.24, 1.15, 1.21, and 1.26 MeV and 23.7, 24.1, 23.9, and 24.6 % per incident neutron for detector 1, 2, 3, and 4, respectively.

**IV.D. NMIS Processor**

The Nuclear Material Identification System (NMIS) processor is a 10-data channel, fast (1 GHz) time correlator that measures (1) the time distribution of events in one detector with respect to a previous event in the

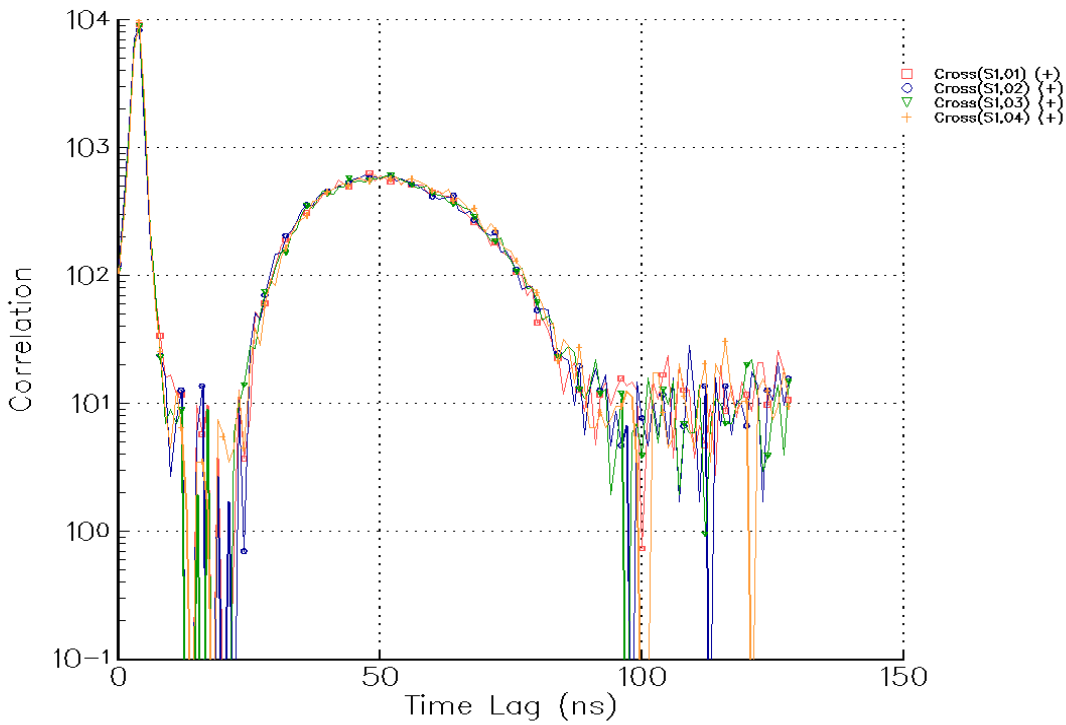


Fig. 4. Typical time distributions of neutrons after Cf fission for the four detectors to determine the detection efficiency as a function of energy.

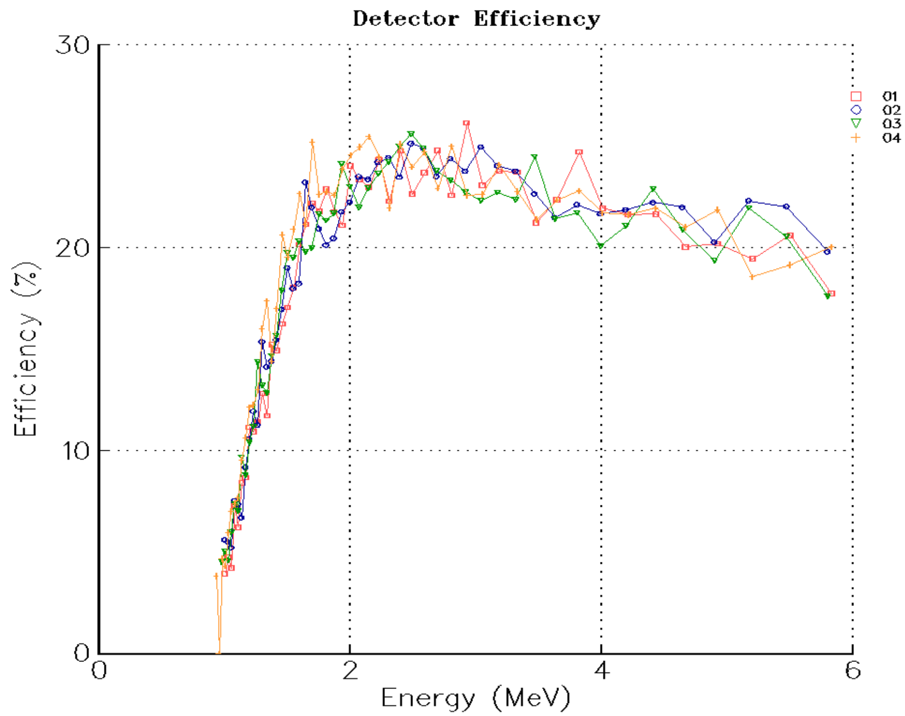


Fig. 5. Typical detection efficiency as a function of neutron energy for four plastic scintillation detectors.

same detector (equivalent to a single detector Rossi-alpha measurement), (2) the time distribution of events in one detector with respect to a previous event in another detector (equivalent to a two-detector Rossi-alpha measurement), and (3) the time distribution of an event in a detector with respect to a time and directionally tagged source event in the alpha detector for the case of a DT generator or time-tagged emission from Cf fission in a parallel plate ionization chamber. For five-channel operation, all these time coincidence distributions are measured simultaneously. In addition, the processor measures multiplets (the number of times a detection event occurs in a time interval), where the time interval is source triggered, detection event triggered, and randomly triggered and time coincidence distributions between any three detection channels including the source.

## V. MEASUREMENTS

### V.A. Measurement Configurations

The source-detector-casting configurations shown in Fig. 6 are (1) a DT generator adjacent to the casting with three detectors, (2) a Cf source adjacent to the casting with three detectors, and (3) the Cf source on the axis of the casting with four detectors adjacent to the casting 90º apart.

A photograph of the Cf source-casting-detector with the Cf source on the axis of the casting is shown in Fig. 7. The DT generator is on the left in the figure and was moved away from the casting when not in use. For the measurements with the generator, the casting was moved on the support table until the steel can with HEU

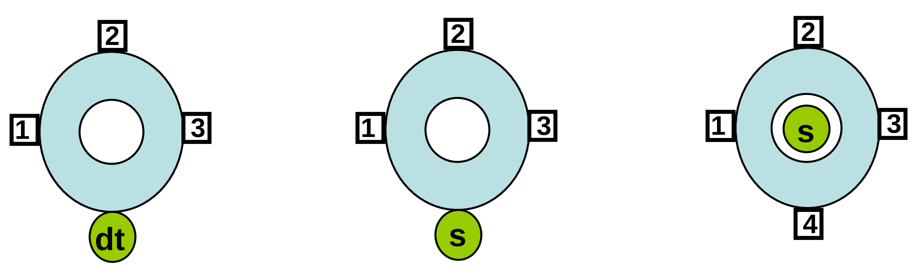


Fig. 6. Source-detector, single-casting measurement configurations and dt designate the DT generator. The numbers indicate detector locations.

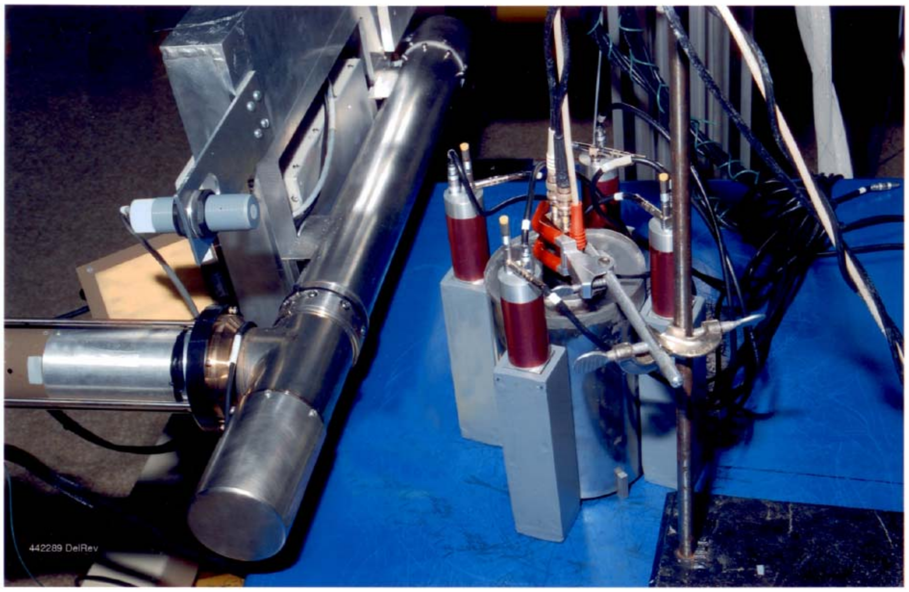

Fig. 7. The Cf source-detector single uranium metal casting with the DT generator on the left and the Cf source on the axis of the casting. The generator is not appropriately positioned for a measurement with the generator as a source.

contacted the DT generator at the longitudinal location of the neutron production spot and three detectors located as shown in Fig. 6. This located the neutron production spot in the generator ~1.5 in. from the casting can.

For these measurements, the center of the casting was 740, 533, 326, and 503 cm from the north, east, south, and west wall of the measurements room, respectively, and the top of the steel table was 102 cm above the floor. The measurements room was 12.8 meters high.

**V.B. Measurement Results**

The time distribution of coincidences between the three detectors and the alpha detection in the DT generator are given in Fig. 8. The measurement time for the measurements with the DT generator was 35 min., with an alpha detection rate of 340,000/s. A portion of detector two is in the time and directionally tagged

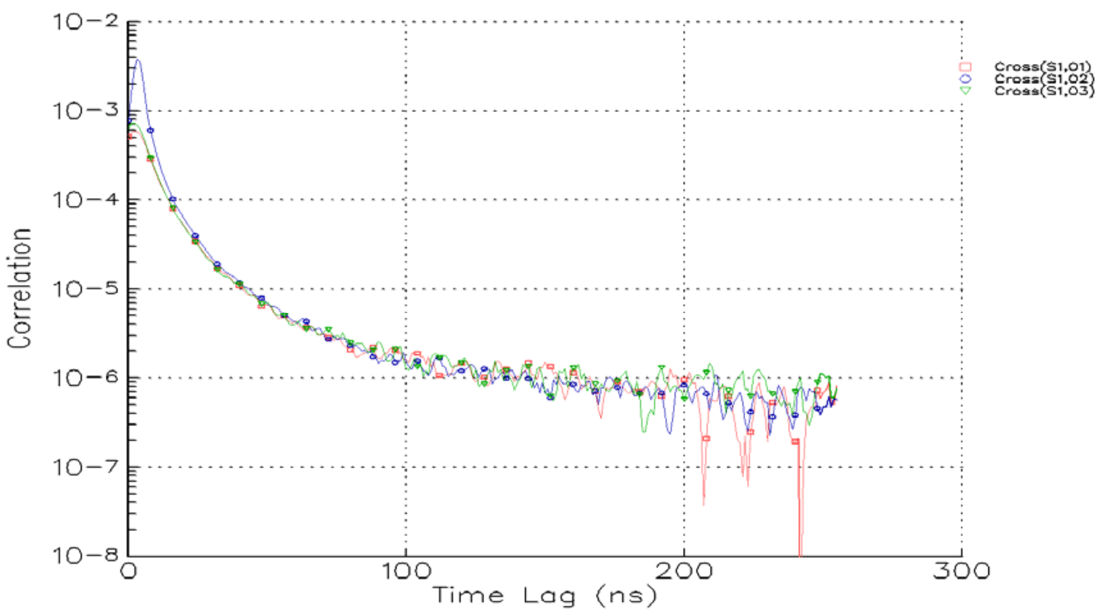


Fig. 8. Time distribution of coincidence count per tagged-source neutron between each of the three detectors and the DT generator neutrons with the source external.

neutron beam from the DT generator and thus has a higher initial detection rate (up to ~5 ns) than the other two detectors, which are at right angles to the source. After the initial source-induced fission, fission chain multiplication emits neutron and gamma rays isotropically, and all three detectors have the same time response after 25 ns. This indicates that the fission chain decay time measured is independent of the detector position. The observed time decay of the fission chains is not exponential as expected because of the low neutron multiplication factor.

The time distributions of coincidences between detectors 1 and 3, 1 and 2, and 2 and 3 are shown in Fig. 9. The different widths of the time distributions are a result of the detectors being different distances from each other: two pairs (1-2, 2-3) with adjacent detectors and one pair (1-3) with detectors on opposite sides of the castings. Except for these small differences, the time dependencies are the same.

The time distributions of coincidences between the three detectors and the external Cf source fission are shown in Fig. 10. The time distribution is not exponential and is independent of detector location after the initial transients associated with detector location. The measurement time was 42 min., with the Cf source external. Similar data for four detectors located 90º apart, as shown in the proceeding photograph, are given in Fig. 11. With an internal Cf source located on the axis of the casting, the time measurement was ~10 min. Again, the time distributions of detector counts after Cf fission are identical because the four detectors are located symmetrically with respect to the source and casting.

The time distribution of coincidences between all detectors with the Cf source on the axis is shown in Fig. 12. Except for small differences near time lag zero, the time dependence is the same for all detector combinations.

The time distributions of coincidences between detectors with the Cf source external are shown in Fig. 13 where the plotted data have been averaged over 5 ns. The time distributions are slightly different: the distribution for detector 1-3 is slightly wider because the detectors are farther apart than the combinations 1-2 and 2–3.

## VI. COMPARISON OF MEASUREMENTS WITH THE TWO SOURCES

Figure 14 shows the time distributions of counts in one of the detectors after alpha detection in the DT generator, after Cf source fission with the Cf adjacent to the outside of the casting can, and on the axis of the casting.

The time distribution of coincidences with respect to the source persists longer for the DT generator because the 14.1 MeV neutrons bounce around the room above the detection threshold longer than they do for the fission energy neutrons from the Cf source. The time distribution of coincidences between detectors one and three for the three measurements is shown in Fig. 15.

The time distribution of coincidences between detectors for the measurements with the DT generator persists longer at long times because of the time and directionally tagged neutrons that pass through the assemblies scattering off the floor and walls of the room.

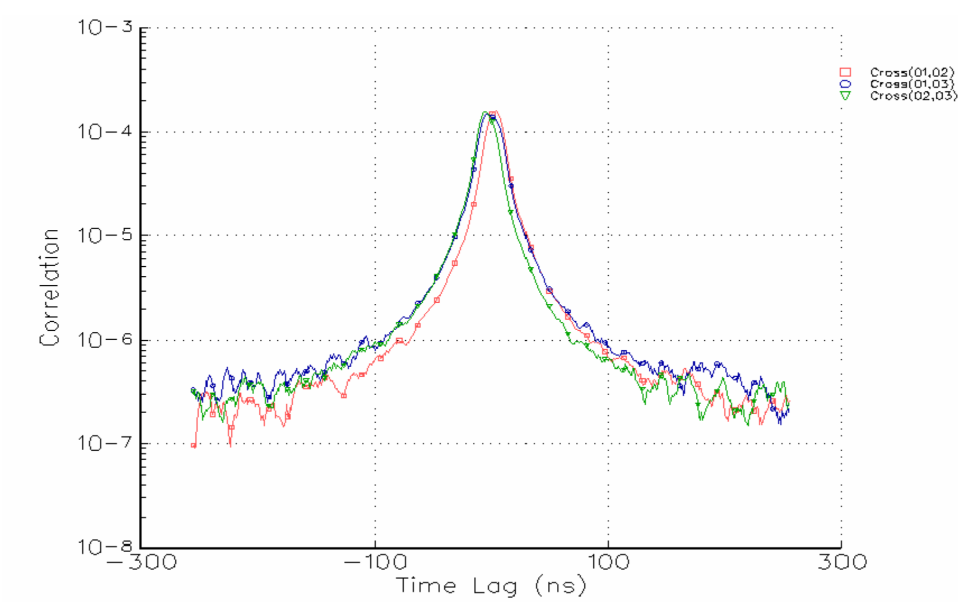


Fig. 9. Time distribution of coincidences between detectors for measurements with an external DT source. The data have been averaged, and all averages are not plotted.

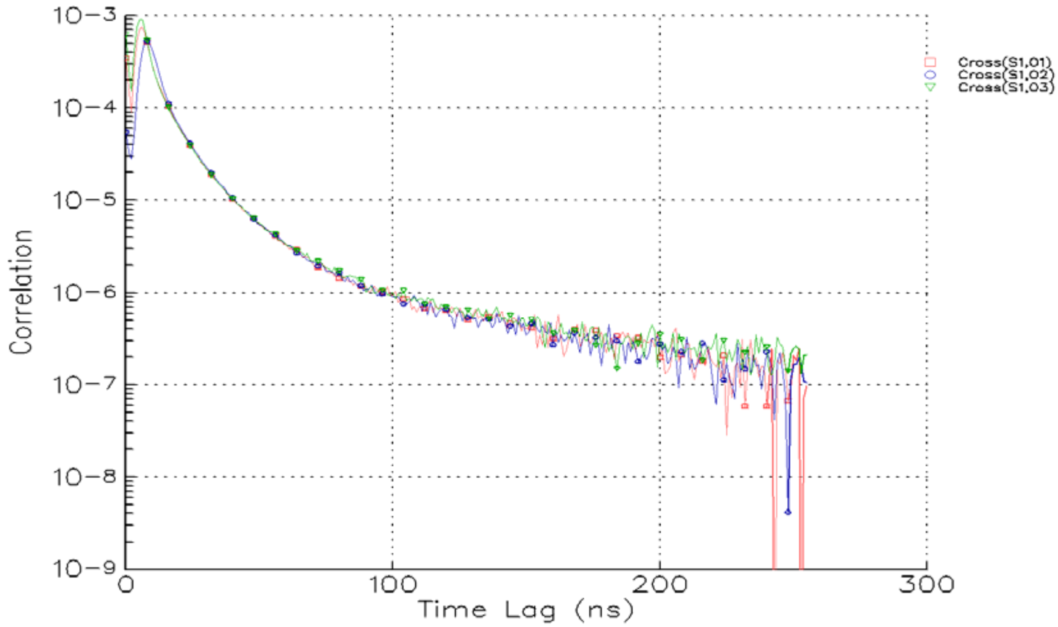


Fig. 10. Time distribution of coincidence count per Cf fission between each of the three detectors and the Cf source fission with an external source.

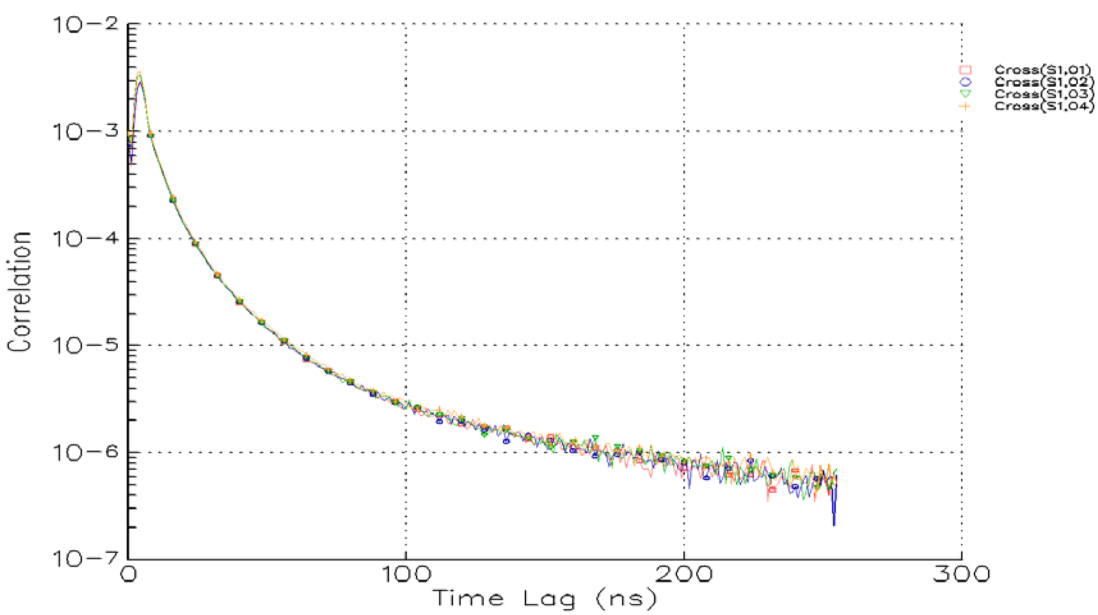


Fig. 11. Time distribution of coincidence count per Cf fission between each of the four detectors and the Cf source fission, with the Cf source on the axis of the annular casting.

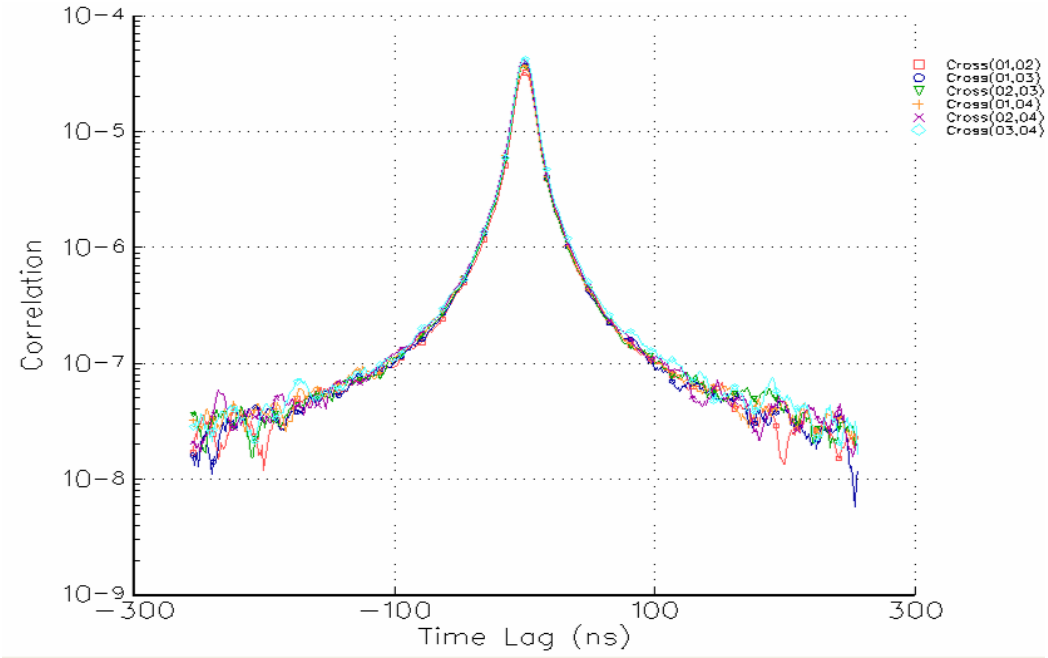


Fig. 12. Time distribution of coincidences between detectors with the Cf source internal. The data on this plot are averaged over five time bins of 1 ns each.

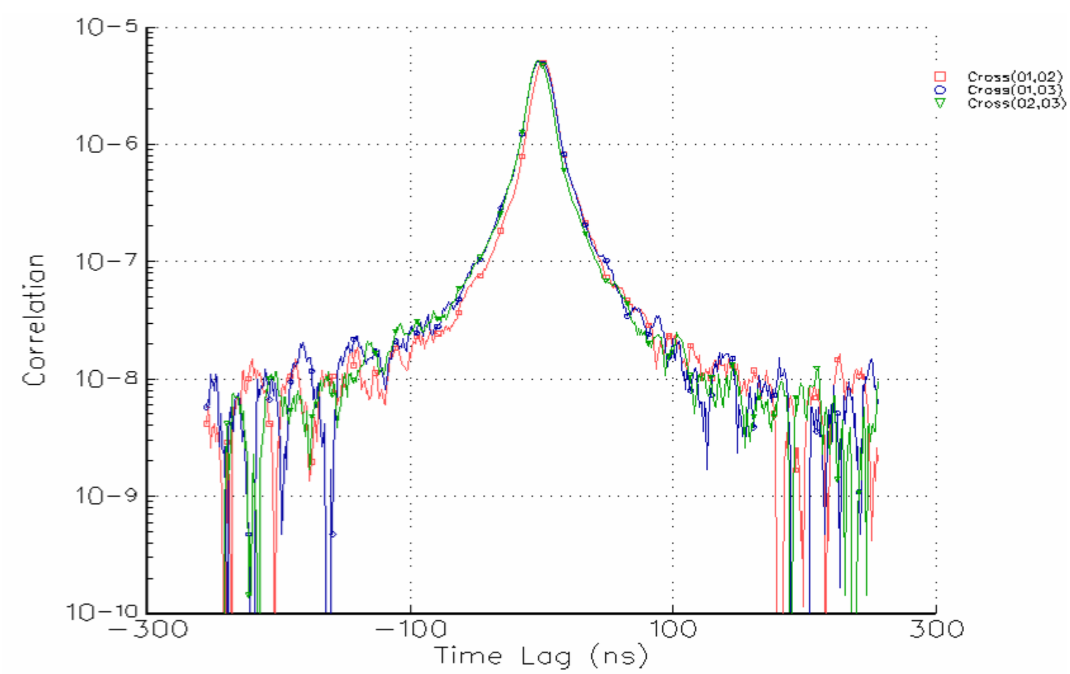


Fig. 13. Time distribution of coincidences between three detectors with Cf source external.

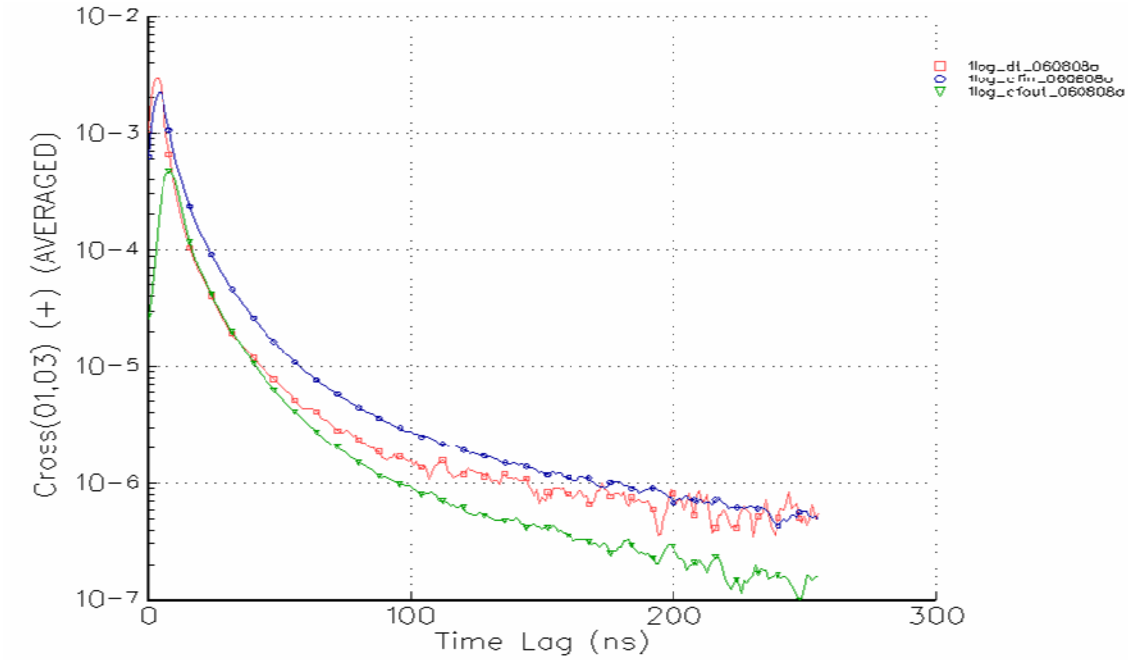


Fig. 14. Comparison of the time distribution of counts in one detector (2) with respect to the source event for the three measurement configurations of Fig. 6.

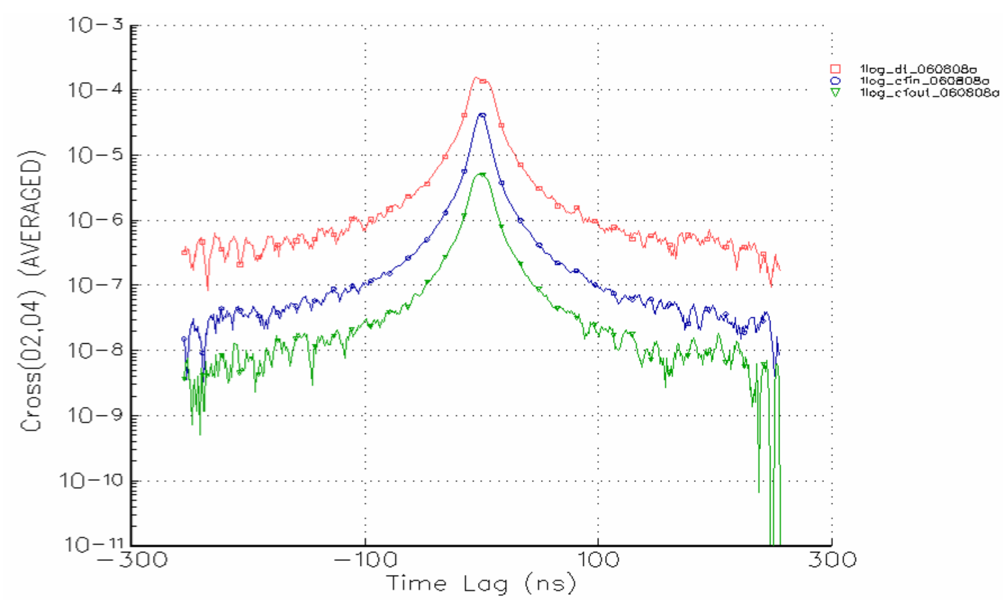


Fig. 15. The time distribution of coincidences between detectors on opposite sides of the casting for the three configurations of Fig. 6.

Thus, when the Cf source is closely coupled to the HEU, the effects of the experimental room on the measured results are less for the Cf source. If the Cf source is some distance from the HEU, the reverse is true. When the source cannot be located adjacent to or inside the fissile material, significant numbers of neutrons from the Cf source scatter from the walls and floor of the room before they reach the fissile material because the time-tagged neutrons go in all directions from the source. Thus, no additional information as to the prompt time behavior of the fission chain multiplication process is provided by the DT generator for measurements with fissile materials where the Cf source can be located inside or in contact with the fissile material. Thus, the use of a DT generator is not necessary for these types of measurements as long as the Cf source can be in or in contact with the fissile material.

## VII. CONCLUSIONS

These data are sufficiently accurate for a well defined experimental configuration that they can be used to benchmark calculational methods for both the time evolution of the fission chain multiplication and the neutron multiplication factor. Measurements with the DT generator closely coupled with the HEU provide no more additional information than those with the Cf source closely coupled with the HEU and are complicated by the time and directionally tagged neutrons from the generator scattering between the walls and floor of the measurements room and the casting while still above detection thresholds.

## REFERENCES


1. J. T. MIHALCZO, J. A. MULLENS, J. K. MATTINGLY, T. E. VALENTINE, "Physical Description of Nuclear Materials Identification System (NMIS) Signatures," *Nucl. Inst. Meth. A*, **450**, 531 (2000).
2. "API120 D-T Neutron Generator User Manual," Thermo Electron Corporation, Colorado Springs, Colorado, www.thermo.com/neutrongenerators.
3. J. T. MIHALCZO, "The Use of Californium-252 as a Randomly Pulsed Neutron Source for Prompt Neutron Decay Measurements," *Nucl. Sci. Eng*., **53**, 393 (1974).